Advanced Synthesis on Lead-Free KNN Piezoceramics for Medical Imaging Applications

Sebastiano Garroni, Nina Senes, Antonio Iacomini, Stefano Enzo, Gabriele Mulas, Lorena Pardo, Santiago-Cuesta Lopez*

Dr. Sebastiano Garroni

International Research Centre in Critical Raw Materials-ICCRAM, University of Burgos, Plaza Misael Banuelos s/n, 09001 Burgos, Spain

Advanced Materials, Nuclear Technology and Applied Bio/Nanotechnology. Consolidated Research Unit UIC-154. Castilla y Leon. Spain. University of Burgos. Hospital del Rey s/n, 09001 Burgos, Spain

E-mail: sgarroni@ubu.es

Nina Senes, Antonio Iacomini, Prof. Stefano Enzo, Prof. Gabriele Mulas

Department of Chemistry and Pharmacy, University di Sassari, Via Vienna 2, I-07100 Sassari, Italy

Prof. Lorena Pardo

Instituto de Ciencia de Materiales de Madrid, CSIC, c/Sor Juana Inés de la Cruz, 3 Cantoblanco, 28049 Madrid, Spain

Dr. Santiago Cuesta-Lopez

International Research Centre in Critical Raw Materials-ICCRAM, University of Burgos, Plaza Misael Banuelos s/n, 09001 Burgos, Spain

Advanced Materials, Nuclear Technology and Applied Bio/Nanotechnology. Consolidated Research Unit UIC-154. Castilla y Leon. Spain. University of Burgos. Hospital del Rey s/n, 09001 Burgos, Spain

KEYWORDS: Piezoceramics, KNN, wet-chemistry, solid-state reactions, Ultrasonic transducer

ABSTRACT

Ultrasonic imaging system is a non-invasive medical imaging technique that has become one of the most widely used diagnostic tools in modern medicine for detecting prenatal anomalies and deep screening of biological tissues. One of the core components of the ultrasound system is represented by the probe where is located the transducer which produces mechanical energy in response to electrical signals, and conversely, produce electrical signals in response to mechanical stimulus. The ultrasound transducer in the probe is generally made of a piezoelectric ceramic material such as lead zirconate titanate (PZT), which present two important limitations as the presence of toxic material as the lead, and low acoustic impedance ascribable to its high density. For these reasons, it is necessary to focus the research on new eco-friendly piezoelectric materials with properties comparable with PZT. Among them potassium sodium niobate is considered as a leading lead-free candidate to replace lead based piezoceramics. Over the years many systems have been studied; among them lead-free $K_xNa_{(1-x)}NbO_3$ (KNN) – based materials, result the most promising. In this review, the most relevant and advanced synthesis approaches and the unique properties of this class of lead-free piezoceramics have been presented in detail.

1. Introduction

Piezoelectric materials have become a key technology for a wide range of industrial and consumer products. Current technology includes applications on actuators, ultrasonic motors, transformers, micro-energy harvesting devices, hydrophones, high resolution ultrasonic medical imaging, and accelerometers in mobile phones and notebooks.[1] In the last two decades, piezo- devices market has seen a tangible growth. The current market was estimated approximately at € 4 billion in 2015 and forecasts indicate that

it would doubled (€ 8 billion) by 2024. [2] In this context, Europe represents the most important piezo-transducer market with € 1.2 billion in 2015 covering the 30 % of the global market. [2]

Piezoceramics is the largest material group for piezoelectric devices, and, currently, the strongest demand comes from ultrasonic transducer for medical diagnostics and therapy - with € 1.8 billion, represents the third largest market in the world - which are gaining ever-increasing importance among piezo-device suppliers. [2]

Different types of ultrasonic transducers, typically working in pulse-echo mode, can be used in medical diagnostical devices. The piezo transducer arrangements can be schematized in the following four categories (Figure 1), depending on the specific body part to be examined:

Single piezo element, reported in Figure 1a, can produce linear scan also in several directions, and it is typically used in the tip of the intravascular ultrasound (IVUS) probes for scanning internal part of the body. For outside, linear array (Figure 1b) and phased array (Figure 1c) arrangements are mostly preferred, because allow to allocate hundreds of piezo elements with a significant gain of the portion examined. Finally, matrix arrays, visualized in Figure 1d, allow to scan a volume and it is extensively used in 3D probes for echography. [1]

In the last years, particular attention has been focused on 3D and new generation 4D ultrasonic transducers (commonly known as medical probes, Figure 2a) widely used to visualize the internal condition of the human body without damaging them including prenatal examinations to which radiography cannot be applied.

An ultrasonic transducer is basically composed by multilayer elements (Figure 2b) including i) a backing substrate which absorbs the acoustic emissions, ii) an active layer made of a piezoceramic disk and iii) a matching layer, typically based of a piezoceramic material but possessing an acoustic impedance approaching that of the investigated tissue. [3-5]

The performance and imaging quality of ultrasonic scanner are highly affected, in large part, by the characteristics (acoustic impedance, piezoelectric performance, dielectric constant, mechanical stability) of the piezoelectric material placed in the active layer. Better sensitivity (-24 dB) and high-frequency (25

MHz) properties could allow to develop a high-efficient 3D/4D probe for prenatal examination able to detect body malformations and pathologies from the early stage of growth. [6] Broadband transducers, operating at multiple frequencies, are typically used in this field. The quality of a transducer analysis, in term of resolution and sensitivity, can be improved transmitting at lower frequencies while receiving the echo signal at higher frequencies. High frequency signal allows to obtain a high imaging resolution while low frequency (higher wavelength), which result in less attenuation, provides a deep penetration into the tissue. The attenuation coefficient, in fact, typically satisfies a frequency power law as indicated in the following empirical equation:

$$\alpha = af^b$$

Where a and b correspond to tissue coefficients. [1]

Finally, a large acoustic impedance mismatch existing between piezoceramics (25-35 MRayls) and body tissue (1.5MrRayls), affects significantly the ultrasound device performance. For this reason, a matching layers elements together with its microstructure and geometry properties, being crucial for developing high performing ultrasonic transducers for medical imaging application. [7]

The most-commonly piezoceramics materials used, the highly-dense PZT ceramics with general formula $Pb(Zr_xTi_{1-x})O_3$, are characterized by high values of density and relative permittivity, which negatively influence the performance and limit their application in the ultrasonic devices. Dense PZT-type materials, in fact, show low hydrostatic figure of merit (HFOM) and poor acoustic coupling to the media with which it is in contact and are therefore not suitable for these applications. [8, 9] On the contrary, porous PZT materials, p-PZT, represent a valid and innovative technological solution, because characterized by low acoustic impedance (Z) value, which reduces the mismatch between the device and the media through which the signal is transmitted or received, leading to a more efficient acoustic wave transfer. [10] Recently, Yang and coauthors, fabricated a porous PZT ceramics with high porosity degree ranging from 31.3% to 58.6%, with interesting HFOM values of 10.117×10^{-15} Pa^{-1}, 1000 times higher than the corresponding dense materials. [11] A large variety of synthesis methods are reported in the current

literature, such as replica technique using synthetic or natural templates, sacrificial template method by liquids, salts, metals, natural and synthetic organics agents and direct foaming methods with different surfactants. [5, 12, 13] In particular, new challenges regard the opportunity to synthesize PZT ceramics with highly 3D interconnected pores and high porosity (> 80%) with the aim to significantly improve the HFOM parameters while maintaining high or promising piezoelectric capacity. Important issues, such as mechanical stability, wettability and poor electric performance remain still unresolved, and represent the main barriers to a rapid commercialization in the international market of the porous PZT ceramics for ultrasonic transducer applications. Furthermore, the presence of a lead-based material can be considered a critical issue for device working in contact with biological tissues.

During the last decades, important efforts have been addressed to the search of high-performing lead-free piezoceramics. [14-17] The replacement of lead-based systems has been considered necessary as a consequence of the ever-increasing number of countries which have banned lead and lead oxide for their toxicity. [17] In 2012, the UE emanated a new directive about the "Waste Electrical and Electronic Equipment (WEEE) and Restriction of the use of certain Hazardous Substances in electrical and electronic equipment (RoHS)". It has been one more time highlighted that lead represents a primary risk during recycling. [18] In this direction, extensive research has been conducted on the development of lead-free piezoelectric materials with properties comparable to the lead-based piezoelectrics such as high piezoelectric coefficient and electromechanical coupling factor. Among these lead-free candidates, in the past 10 years, $K_xNa_{1-x}NbO_3$ (KNN) has become one of the most investigated lead-free piezoelectric system due its large d_{33} (~390-490 pC/N) and relatively high Curie temperatures, T_C, (~217-304 °C), coupled with its high chemical inertia and compatibility with human tissue, which made it optimal for human diagnostic devices. [19-23]

Modification of morphotropic phase boundaries (MPB) is a classical standard route in the field of piezoelectric materials used to improve its properties, where the crystal structure changes as a function of composition makes possible the coexistence of polymorphs for a given composition. [24] In the KNN-

system, the properties depend not only on the phase composition but also on the temperatures among the intrinsic characteristics of polymorphic phase transition (PPT).

$K_xNa_{1-x}NbO_3$, in the composition x = 0.5 close to the MPB, is a solid solution of ferroelectric $KNbO_3$ and antiferroelectric $NaNbO_3$ whit perovskite structure. [25] At room temperature presents an orthorhombic crystal structure (Figure 3) and two phases transitions at higher temperatures: orthorhombic to tetragonal (O-T) at 200°C and tetragonal to cubic (T-C) at T_C 420°C.

Above this temperature, the sample loses the piezoelectric propriety. [27-29] Despite the interest, this system suffers of several disadvantages: pure ceramic KNN are difficult to be obtained by conventional synthesis method due to the volatility of the alkali components, instability of the crystalline phase at high temperature and extremely narrow sintering-temperature range. [30, 31] Furthermore, the presence of KNN grains with cubic shape decreases the packing efficiency whit a drastic reduction of the disk density.

Another widely used method was the chemical modification through doping with additives (e.g., ion substitutions, binary or ternary solid solutions, etc.). This approach allows to improve the sintering behaviour of KNN, while keeping its inherent structure and phase diagram and improving specific properties like piezoelectric coefficients or coupling constants. [32-34] Furthermore, its doping with specific elements allow to decrease the orthorhombic-to-tetragonal phase transition in KNN from 200 °C (pure material) to near or below room temperature. [35, 36] The pioneer work of Saito et al. has promoted an extensive research on this system: KNN doped with Li, Ta and Sb ions, showed interesting piezoelectric constants d_{33} of 400 pC/N and a Curie Temperature of 253 °C. [15] Recently, Zhang and Rubio-Marcos groups obtained a large d_{33} of 400 pC/N by the modification of the rhombohedral–tetragonal (R–T) phase boundary and domain structures. [37, 38] The formation of the R-T phase boundary may become necessary to further enhance the piezoelectric activity and narrowing the gap between lead-free and lead-based materials. [39, 40] Indeed, the addition of ions or ABO_3 materials could simultaneously increase $T_{R\text{-}O}$ and decrease $T_{O\text{-}T}$ of KNN materials, favouring the $T_{R\text{-}T}$. [41, 42]

Recently, three main preparation procedures were emerged for the KNN synthesis, which involve the i) solid-state or conventional routes (SSR), ii) crystal growth used for fabricate large single crystals and

iii) wet chemistry routes such as sol-gel, solvothermal, Pechini, hydrothermal, etc. If the SSR route has been considered a fast and solvent-free procedure to produce KNN pellets, the exploitation of the wet-chemistry methods allowed to significantly improve the control of the stoichiometry in the final system. In fact, soft conditions, typically used in the wet-chemistry methods, permits to overcome critical problems, well known in the high temperature SSR reactions, related with the low-melting components.

In this review, the most recent and appealing results on the KNN piezoceramics are presented and discussed in detail. Particular emphasis is placed versus the emerging and advanced procedures, solid state and wet chemistry routes, enable to influence and drastically improve the piezo properties of the KNN materials and, as future perspective, to modulate the porosity in the mesoporous region. The properties are expressed by interrelated coefficients, as the piezoelectric charge constant d_{ij}, density, Curie temperature *Tc*, dielectric constant, frequency, and the electromechanical coupling coefficient *k*, in order to better compare the performance of the systems here reported and then identify promising candidates useful in devices for biomedical applications.

2 Advanced Synthesis and Properties of KNN and related compositions

2.1 Dense KNN prepared by conventional route

KNN presents three phase boundaries corresponding to approximate values of x = 0.17, 0.35 and 0.5, although much attentions were addressed to the system with x = 0.5 value. The stoichiometric control and MPB are key factors for obtaining good piezoelectric properties and these aspects can be tuned through different preparation techniques.

Despite their promising properties, KNN-based piezoelectric are still not widely used in industrial product. The main drawbacks reported in the current literature are related with the difficulties to obtain high densities of sintered products and in controlling its microstructure, together with deviations from the stoichiometry and the subsequent formation of secondary phases. [31] These problems, as introduced in the introduction section, can be accredited to the high volatilization of alkali elements at sintering temperature, which is typically higher than 1100°C. [43] The piezoelectric activity of KNN materials can

often be enhanced by increasing their density and is also very sensitive to fluctuation of composition when the compositions are situated at the phase boundary regions. [44]

Solid state reaction route is the common way to synthesize KNN and it consists of different steps summarized in Figure 4.

Mixing step can be performed simply using a mortar and pestle, with a raw dispersion of the powders involved in the process, or by high-energy ball milling which allow to better refine the crystallite and particle dimensions, and activate the solid-state reaction until the calcination process.

Sodium carbonate, potassium carbonate and niobium oxide are typically used as starting materials, although other alkali compounds such as nitrate, hydrogen carbonates or sodium potassium tartrate hydrate have been similarly exploited. [31] The summary reaction with alkali carbonates and niobium oxide is describe by the chemical equation (1) and, according to the thermogravimetric analysis, it occurs between 750 and 950°C. [31]

$$K_2CO_3 + Na_2CO_3 + 2\,Nb_2O_5 \rightarrow 4\,K_{0.5}Na_{0.5}NbO_3 + 2\,CO_2 \qquad (1)$$

Birol et al. reported a process to synthesize KNN pellet with a theoretical density of 95%, by sintering the alkali carbonates and niobium oxide reagents up to 1114°C for 2 hours in oxygen rich atmosphere. [45] These systems reported an electromechanical coupling coefficient, k_t, in the thickness direction, of 45%., whereas the piezoelectric coefficients in longitudinal and planar directions are d_{33} = 100 pC/N and d_{31} = 43 pC/N, respectively. These values result quite promising, although still too low if compared with typical PZT ceramics (d_{33} = 400 – 700 pC/N).

Numerous attempts have been made in order to improve the piezoelectrical properties and density of KNN by using metal oxides as dopants. Zuo et al., for example, investigated the effect of La_2O_3, Fe_2O_3 and La-FeO_3: the addition of small amount of Fe_2O_3 or La–FeO_3 promotes densification and increases ferroelectric and piezoelectric properties. [46] On the other hand, La^{3+} doping tends to cause poorer densities, and thus extremely high loss tangent values. Doped KNN ceramics obtained by ordinary

sintering, can reach a piezoelectric constant d_{33} of 145 pC/N and a coupling factor k_p of 43%. Rödel et al. compared the influence of various oxides as ZnO, SnO_2, Sc_2O_3 and CdO. [47] These oxide-doped KNN samples reported an improved sintering behavior coupled with good electromechanical properties. In particular, d_{33} = 117 pC/N and k_p = 44%, and d_{33} = 108 pC/N and *kp* = 39% values, were achieved for the ZnO- and SnO_2-doped samples, respectively. In order to further improve the sinterability, CuO is often used due its low melting point and liquid phase formation. [48] Saito et al., obtained a KNN based piezoelectric doped by CuO in the sintering process, with high relative density of 98,9% and very promising electromechanical properties. [15] Su found that the addition of 1 mol% CuO and 1 mol% SnO_2 at 1070 °C improved dielectric and piezoelectric properties in comparison with the un-doped system. [49] On the basis of these evidences, Yang et al. studied the dependence of doping amount of $CuNb_2O_6$ on piezoelectric and ferroelectric properties of KNN. [48] The results showed that the CN-doped KNN specimens, sintered at 1075 °C, presented an excellent "hard" piezoelectric properties of k_{33} = 92.5 coupled with an extraordinarily high mechanical quality factor (*Qm*) of 1933.

Copper based sintering additives such as $K_4CuNb_8O_{23}$ (KCN) and $K_{5.4}Cu_{1.3}Ta_{10}O_{29}$ (KCT) were also found to be very effective in improving the sinterability of KNN-based ceramics. [43] Lin and Chul used the KCT with MnO_2 and CuO: KNN-Mn-KCT system shows good piezoelectric properties (d_{33} = 90 pC/N and *kp* = 40%). [50,51] Because of the 'pinning' effects provided by the defect dipoles, the ceramic becomes 'hardened', exhibiting a high *Qm* (1900) and a low ε_r (300); while CuO doping of the KNN–KCT ceramics improved the *Qm* up to 3053. It is suggested that there is a transition in the doping behavior of Cu ions in KNN–KCT ceramics. At low doping levels (x < 1.0), Cu ions seem to substitute pentavalent B-site cations, acting as acceptors that generate O-vacancies to harden domain reorientation. However, Cu ions play a role as donors by replacing A-site cations at high doping level (x > 1.5).

A further attempt to lower the sintering temperature was made by Bernard et al. [52] The densification of KNN ceramics has been improved by the addition of small amount (from 0.5 to 4 mass %) of (K, Na)-germanate, which melts at around 700°C. Germanate-modified KNN ceramics can be sintered reaching high density (95.6 %) at 1000°C, which is more than 100°C lower than that usually required for pure

KNN. The addition of a sintering aid not only improves the densification but also preserves the good piezoelectric properties of KNN.

Li^+, Sb^{5+} and Ta^{5+} are well-known doping elements, which are able to quickly shift the orthorhombic-tetragonal phase boundary at near room temperature, resulting in an enhanced d_{33} value. For example, the introduction of Li^+ into KNN allowed to increase the Curie temperatures and decrease the *To-t*., while maintaining a good piezoelectric constant. Additionally, the sintering temperature was decreased and the density of the final pellet significantly improved. [44] Song et al. studied, in detail, the (1-x)KNN–xLN system in the MPB range x = 0.05-0.08. [53] Good piezoelectric properties were obtained at x = 0.07 for the specimens sintered at 1030°C and subsequently annealed at 1050°C. For these samples, evaporation of Na_2O was observed during the sintering step. Wang et al. studied the same system using excess of Na_2O. [54] They found that the crystal structure changed from orthorhombic to tetragonal with increasing $LiNbO_3$ amount since the phase transition temperature T_{O-t} shifted downward. In the region of two-phase coexistence (x = 0.08), enhanced piezoelectric constant d_{33} (280 pC/N) and electromechanical coupling factor k_p (48.3%) with a high Curie temperature *Tc* (475 °C) were obtained using low sintering temperature (950°C); therefore, excess of Na_2O could effectively reduce sintering temperature which is reflected in better piezoelectric properties.

Perovskite ABO_3 materials are often used to modify KNN in order to induce enhancement in piezoelectric activity by favoring the formation of phase boundaries. [44] Among them, $Bi_{0.5}A_{0.5}TiO_3$ (A= Na^+,K^+,Li^+), $BTiO_3$ (B = Ba^{2+}, Sr^{2+}, Ca^{2+}) and $(Bi_{0.5}Na_{0.5})_{0.94}Ba_{0.06}TiO_3$, presented the most priming activity. For example, Su et al. studied the $(1 - x)(K_{0.5}Na_{0.5})NbO_3$–$x(Bi_{0.5}Na_{0.5})TiO_3$ (KNN-BNT) systems. [55] They reported the formation of a pure perovskite phase with orthorhombic symmetry at $x < 0.02$, tetragonal symmetry at $x > 0.03$ and the coexistence of orthorhombic and tetragonal phases in the range $0.02 < x < 0.03$. In this composition, the system shows the best piezoelectric properties (d_{33} =~ 256 pC/N, d_{31} = 85 pC/N, *k*p = 48%, *k*t = 0.52 and *T*c = 373 °C). Lead-free ceramics $(1-x)(K_{0.5}Na_{0.5})NbO_3$–$xBa(Zr_{0.05}Ti_{0.95})O_3$ doped with 1 mol % MnO_2 have been studied by Lin et al. [56] These system shows good properties due to a coexistence of the orthorhombic and tetragonal phases at room temperature

between 0.04 < x <0.07. The ceramic with x = 0.06 exhibits the following optimum properties: d_{33} = 234 pC/N, kp = 49%, kt = 48%. KNN doped with $(Bi_{0.5}Na_{0.5})_{0.94}Ba_{0.06}TiO_3$ (BNBT) [57] showed very similar properties with respect to the KNN-BNT system. [54] A different system such as $Bi_{0.8}La_{0.2}FeO_3$ (BLF) was studied by Zhang et al. [58] In this work, the addition of small amount of BLF increased the piezoelectric properties of KNN but not significantly with respect to BNT and BNBT systems.

As emerged from the specific literature, many works have been carried out in order to build two kinds of phase boundaries (O-T and R-O), however the d_{33} values of R-O and O-T KNN based ceramics are still poorer compared to the lead based ones. The PZT, for examples, shows the best properties at the MPB where coexist the rhombohedral and tetragonal phases which leads to a large d_{33} constant and weak temperature dependence. [44] On the basis of this observation, several authors have tried to build the R-T phase boundary in KNN systems by lowering the T_{O-T} and increasing the T_{R-O} to room temperature. Some additives were able to decrease the T_{O-T} to room temperature like $LiBO_3$ (B = Nb^{5+}, Ta^{5+}, Sb^{5+}) or $CTiO_3$ (C = Ba^{2+},Sr^{2+},Ca^{2+}) while additives such $DZrO_3$ (D = Ba^{2+},Sr^{2+},Ca^{2+}) and $BiEO_3$ (E = Sc^{3+}, Al^{3+}, Fe^{3+}, Co^{3+}), Ta^{5+} and Sb^{5+}, can shift T_{R-O} to room temperature. [43]

Zhang et al. have studied $0.96(K_{0.5}Na_{0.5})_{0.95}Li_{0.05}Nb_{1-x}Sb_xO_{3-0.04}BaZrO_3$ system; The rhombohedral−tetragonal phase boundary has been identified in the composition range of $0.04 \leq x \leq 0.07$. [59] The ceramic with x = 0.07 has a giant d_{33} of ~ 425 pC/N, which is comparable to that (~ 416 pC/N) of textured KNN-based ceramics, however possess low Tc value (197°C). Cheng et al developed a lead free piezoelectric system based on $(1-x)(K_{0.48}Na_{0.52})(Nb_{0.95}Sb_{0.05})O_3$- $xBi_{0.5}(Na_{0.7}K_{0.2}Li_{0.1})_{0.5}ZrO_3$. [60] The coexistence of a tetragonal phase and a rhombohedral phase is identified in the composition range of 0.03 < x < 0.05. For such composition, the ceramics showed very high d_{33} of 380 pC/N, high Tc of 290 °C, and a good thermal-depolarization behavior of 210 °C.

In table 1, the properties of the here discussed KNN systems are summarized.

2.2 KNN in ultrasonic applications

The development of technology for improving ultrasound imaging of human tissues, is now oriented versus ultrasound transducers with an operational frequency ranging from 30 to 50 MHz. Along this direction, many efforts have been addressed to the preparation of KNN-based systems with an equivalent or better piezoelectric performance with respect to the lead-based ones.

For this purpose, a limited number of synthesis routes have been proposed. In particular, technics to prepare large crystals (mm) were exploited for a direct application. In a recent paper, a new technique similar to the top-seeded solution growth (TSSG_Figure 5 a) allowed to obtain complex stoichiometry without contamination. This procedure, called floating zone method (FZM_Figure 5 b), was used to prepare KNN large crystals (Figure 6 a) doped with Mn and Ta. [61]

The sample presented promising properties such as k_t of 48% and d_{33} of 70 pC/N, interesting for ultrasonic devices. For this reason, a similar system was used to fabricate a high-frequency intravascular ultrasonic probe: the lead-free KNN–KBT–Mn (0.4%), $0.97K_{0.5}Na_{0.5}NbO_3$–$0.03(Bi_{0.5}K_{0.5})TiO_3$ showed a center frequency, bandwidth, and insertion loss of 40 MHz, 72%, and 28.8 dB, respectively. [62] Further improvements have been achieved with the $0.96(K_{0.48}Na_{0.52})(Nb_{0.95}Sb_{0.05})O_3$–$0.04Bi_{0.5}(Na_{0.82}K_{0.18})_{0.5}ZrO_3$ ceramic system, KNNS-BNKZ, which presented an extremely high d_{33} of 490 pC/N allowing to successfully fabricate a 37-MHz high-frequency ultrasound transducer. The sample, fabricated by conventional solid-state, can compete with that of commonly used PZT-based ceramics and could represent a good candidate for lead-free high-frequency ultrasound imaging. [63] Previous studies, conducted by Hagh at al. showed that the KNN-LT-LS ceramics, $K_{0.5}Na_{0.5}NbO_3$-$LiTaO_3$-$LiSbO_3$, doped with 1 mol% Ba^{2+}, can be efficiently used to fabricate single-element ultrasonic transducers resonating at 5.5 MHz. [64] These new donor doped solid-solution systems were prepared by conventional wet ball milling, using acetone as medium and potassium, sodium and barium carbonates, and niobium, tantalum and antimony oxides, as reagents. The system doped with 1% of barium exhibited an orthorhombic crystalline structure, a piezo constant, d_{33}, of = 210 pC/N and a $\varepsilon^T_{33}/\varepsilon^0$ of 1173 (1kHz). Huo and coauthors

prepared a Li, Ta- modified KNN single crystal (Figure 6 b), via top-seeded solution growth (TSSG) method. [65, 66] The crystals were grown along the $[001]_c$ direction and showed a large longitudinal electromechanical coupling factor k_{33} ~ 83% and a piezoelectric response of 255 pC/N, similar to that obtained for the same system prepared by conventional sintering. [67] Finally, interesting electromechanical coupling coefficients (k_{15} = 0.448, k_t = 0.67) were achieved by Tian et al., which investigated a new stoichiometric system $K_{0.8}Na_{0.2}NbO_3$ single crystal using TSSG method. [68]

Despite the fervent interest in the preparation of large crystal for piezo device application, the exponential growth of the microelectronic market recorded in the last 20 years, has moved the attention to the preparation of piezoceramics in smaller size. In this scenario, the thick films of dielectric and piezoelectric materials have been considered optimum candidates to replace the components currently used in bulk ceramic form. Thin films of KNN are typically prepared by physical and chemical methodologies such as magnetron sputtering, pulsed laser deposition (PLD), sol-gel process and chemical solution deposition (CSD).

Levassort et al., prepared a transducer (Figure 7 a) for medical imaging based on a lead-free thick film. [69] The KNN thick film, sintered at relative lower temperature of 200°C, were deposited using a pad printing technology on the electroded backing also made by KNN. The piezoelectric coefficient measured was equal to 80 pC/N and a center frequency over 10 MHz and a –6dB bandwidth close to 93% were observed for the transducer. The in vivo human skin images obtained using this transducer were comparable, in terms of sensitivity, to that recorded with a PZT-based transducer.

Encouraging results were also obtained by Shen at al. which fabricated a transducer (Figure 7 b) using a tick film doped with lithium and tantalum (50 μm) of KNLNT prepared by spark plasma sintered (SPS) technology, schematized in Figure 8 a. [70] Compared to the previous system the SPSed KNLNT ceramic presented a higher operating centre frequency of 29 MHz. To this regard, López-Juárez and co-authors also proved that SPS preparation can be useful for improving the piezo properties of KNLNT. [71] The positive effect is probably ascribable to the lower temperature of sintering and the higher density achieved with respect to the conventional pressureless (PLS) techniques. Similar performance was obtained by the

same authors but using a spray drying technique which allow to obtain small particle size of KNLNT at low sintering temperature. [72]

A valid and cheaper alternative to the SPS technique for preparing KNN tick film, is represented by the electrophoretic deposition method (EPD – Figure 8 b). KNN thin film, with thicknesses ranging from 10–60 μm, was synthesized by EPD method and deposited with acetone and triethanolamine (TEA) as suspension media. The sample showed relative permittivity of 393, dielectric loss about 0.07 and piezoelectric response of 40 pC/N. [73]

A very high-frequency transducer (> 300 MHz) was fabricated using the lead-free $K_{0.5}Na_{0.5}NbO_3/Bi_{0.5}Na_{0.5}TiO_3$ (KNN/BNT) composite thick films synthesized by sol-gel route. The frequency measured, the highest value for a lead-free piezoceramic (170 to 320MHz), can compete with high frequency PZT based transducers. [74] Another system that can be considered a good candidate for ultrasonic transducer is the multilayer KNN ceramic doped with Li, Sb, Ta, prepared by conventional route. [75] Although its remarkable apparent dynamic response of 1839 pm/V, the resonance frequency of 131.8 kHz resulted late for practical application.

The main properties of the system described in this chapter are summarized in table 2.

2.3 Novel KNN-based systems prepared via wet-chemistry.

The high temperature calcinations combined with the prolonged isothermal annealing used in the conventional method for preparing KNN ceramics, results in considerable loss of alkaline elements. For these reasons, the so-called wet-chemistry routes have gained increasing attention in the last years. This approach, in fact, offers several advantages in terms of exact chemical stoichiometry, uniform doping, lower crystallization temperature, high purity and reduced costs. Among them, sol–gel (Figure 9) represents a simple and common synthesis route that can be exploited successfully for synthesizing KNN in nanostructured conditions such as nanopowders, nanorods, nanofibers and thin films.

As demonstration of its feasibility, modified sol-gel routes were recently used to prepare, at low temperature > 600°C) lead-free KNN thin films (~ 100 nm) with enhanced electrical and mechanical properties. [76, 77] Another interesting example, is represented by Kakimoto and co-workers which

synthesized porous $Li_{0.06}(Na_{0.5}K_{0.5})_{0.94}NbO_3$ (LNKN-6) and the composite LNKN-6/$KNbO_3$ using phenol resin fiber (Kynol^{TM}) as templating agent. [78] Due to the low temperature required in the annealing step, the loss of alkali was completely suppressed in this synthesis. Concerning the electric properties, the dielectric loss value of the porous system was comparable with that of the composite, varying from 0.030 to 0.038 independently from the porosity. On the other hand, the dielectric and piezoelectric constants were differents depending on the pores shapes and connectivity. The LNKN-6/$KNbO_3$ composites prepared using 30 vol % Kynol^{TM} showed a piezoelectric coefficient (g_{33}) of 63.0×10^{-3} Vcenterdotm/N, twice than reported for the monolithic LNKN-6 ceramics. [78] As a further example of sol-gel processing used for preparing lead-free piezoelectrics, Li and co-authors showed the manufacturing of KNN microrod arrays using Si mold as templating. [79] The solutions were composed by potassium and sodium ethoxide prepared by the direct reaction of the metals Na and K with ethanol and mixed in 2-methoxyethanol. In this specific case, acetic acid and acetylacetone were used as chelating ligands.

Soderlin et al., described the synthesis of thin films KNN using three different sol-gel methods: alkoxide (I), modified Pechini (II) and a novel oxalate method (III). Only the Pechini-type was useful to obtain a single pure phase (< 600°C), while in the other two cases extra peaks were observed in the corresponding XRD patterns (Figure 10). [80]

Along this line, Chowdhury and co-authors reported the synthesis of the KNN via Pechini method, using an aqueous solution of potassium and sodium nitrate and ammonium niobate oxalate. The nanopowders calcined at 700°C well crystallized with a pseudo-cubic space phase and any trace of secondary phases was observed. The SEM micrographs indicated a particles dimension of 50-150 nm. [81] Pure KNN with a cube-like structure was also synthesized starting from potassium and sodium carbonate, niobium hydroxide and three different chelating agents: citric acid, ethylene glycol and ethylenediaminetetraacetic acid (EDTA). [82] Recently, natural gel was used as stabilizer agent for obtaining KNN nanoparticles at low calcination temperature. [83, 84] The starting materials were sodium and potassium nitrate, ammonium niobate (V) oxalate hydrate, and gelatin type B and starch as stabilizers agents. The TEM image showed that the particle sizes were around 50-100 nm and 20-60 nm for the

samples stabilized by gelatin type B and starch, respectively. Zhang at al. investigated the direct effect of oxalic acid, ethylene glycol and pH in the stability of precursors. It emerged that 750° C was the optimal temperature to ensure a better crystallization and singular phase formation. The grain dimensions obtained for the KNN powders were 100–200 nm. [85] On the other hand, big crystals of KNN can be obtained via sol-gel synthesis starting from nanoparticles and nanorods. [86] This method, also called abnormal grain growth method (AGG), was used to prepare, at 950 °C, single crystals orthorhombic KNN with size of about 3 mm. Biocompatible KNN nanofibers were produced via sol gel combined and deposited via electrospinning, starting from sodium and potassium acetate, niobium ethoxide as reagents and acetic acid as solvent and chelating agent. Interesting, the crystalline nanofibers with a length of 100 µm and diameter 50-200 nm, at room temperature, displayed a spontaneous polarization. [87] Further results, published in a second step, showed that the piezoelectric coefficient d_{33} of these nanofibers was strongly anisotropic varying from 75.8 to 18.3 pm/V for out-of-axis and on-axis oriented ferroelectric domains, respectively. [88]

Further enhancement was achieved by adding other metals to KNN systems via soft chemistry. For example, the piezoelectric constant of nanofibers (see HTEM in Figure 11) increased roughly 5 times when the system was doped with Mn. The 3%Mn-KNN sample showed a d_{33} of 40.06 pm/V and a good mechanical stability and flexibility with voltage and current values of 0.3 V and 50nA, respectively. [89] At the same time, promising candidates, Li-, Sb- and Ta-modified (K, Na)NbO_3 (LTS-KNN) ceramic was synthesized via economical sol gel route. [90] The crystalline powders at room temperature showed a d_{33} of 311 pC/N and a dielectric loss of 0.024.

KNN thin films were prepared via sol gel processing on Nb:$SrTiO_3$ substrate, with different crystallographic orientation by an alkoxide solution : sodium, potassium ethoxide and niobium penthaethoxide in 2-methoxiethanol as solvent and acetilacetone as chelating agent. The large piezoelectric response was obtained along [001] direction with an average local piezoelectric coefficient of 50.5 pm/V. [91, 92] Solarte at al. reported a common synthesis with alkoxide precursors of K, Na and Nb with acetone and ethanol as stabilizer and solvent. These films showed promising piezoelectric properties

especially when the films were modified with Li and Ta. The addition of these dopants improved the polarization: the sample with 5% of Li presents a polarization of 16 μC/cm^2 at 700 °C. [93] Bruncková and co-workers presented the deposition effect of $K0._{65}Na_{0.35}NbO_3$ thin film in different substrates. The technique used is a modified sol gel starting from sodium and potassium acetate, and the Nb-tartarate complex. The system was prepared by spin-coating method on Pt/Al_2O_3 and $Pt/SiO_2/Si$ substrates at 650°C. Uniform morphology and spherical particles of about 50 nm, a lower roughness of 7.5 nm and lower elastic modulus were found in the $Pt/SiO_2/Si$ substrate. [77] The similar sol gel synthesis with niobium ethoxide as precursor and 1,3 propanediol as solvent that bridging ligand to crosslink the ions and generate the network. The most performing sample treated at 500/600°C, showed a remnant polarization, a coercive field of 214 kV/cm and electric field of 150 kV/cm. [94] Yao et al., use the same method but starting from different metallic precursors. This investigation showed that with an excess of K ions, a better ferroelectric activity can be achieved, while the excess of Na played an important role in the improving the dielectric property of the system. [95] The same group synthesized a KNN thin film by citrate complexing sol-gel route. The gas released during the calcination at 450°C, generated a significant porosity degree with pore dimensions of 10-20 nm. However, the ferroelectric properties were improved only when the system was heated upon 550 °C. [96] Dielectric properties could be modulated in KNN system by doping with amphoteric elements. [97] Yttrium, depending on the concentration, can replace ions in the A- or B-site. It has been demonstrated that when the yttrium occupied A-sites, the dielectric loss changes from 0.18% to 0.012%. On the other hand, at higher yttrium concentration, occupying B-sites, a porous system was formed and the dielectric properties significantly increased. Addition of manganese as dopant showed significant benefits also in KNN-modified ceramics prepared by sol-gel route. Recent studies demonstrated that the 2.0% of Mn in the KNLN stabilized the orthorhombic-tetragonal phase boundary at room temperature and high constants d_{33} (212 pC/N) and FOMoff (4.03 x 10^{-10} m^2/N) were obtained. [98]

Hydrothermal method was also exploited to produce KNN materials. The synthesis of $K_xNa_{1-x}NbO_3$ was studied as a function of KOH/(KOH + NaOH) ratio and hydroxide concentration (2–8 N) starting

from Nb_2O_5 as niobium source. $K_{0.02}Na_{0.98}NbO_3$ and $K_{0.1}Na_{0.9}NbO_3$ phases were obtained, proving the difficulty of potassium to become part of the lattice. Additionally, for hydroxide concentration below 2 N, any K^+ rich phase has been detected. This could be ascribable to the dissolution of Nb_2O_5 which is strongly influenced by the pH, temperatures and solvent. [99] With higher hydroxide concentration (8N), the system revealed interesting properties such as a density of 4.33 g/cm^3, a loss tangent of 0.03 with a coercive electric field of 31 kV/cm, a saturation polarization of 16 μC/cm^2 and high remnant polarization of 11 μC/cm^2. In order to avoid agglomeration and improve the physical density after sintering, surface modifiers such as cetyltrimethylammonium bromide, hexamethylenetetramine, and Triton X-100, have been introduced in the abovementioned hydrothermal synthesis. [100] Using this modification, the $K_xNa_{1-x}NbO_3$-based ceramics exhibited enhanced electrical properties showing d_{33} of 61 pC/N, loss dielectric ranging from 0.037 to 0.028 and real permittivity around 400. A typical hydrothermal route was used to prepare KNN doped with diverse amount of Sb ($K_{1-x}Na_xNb_{1-y}Sb_yO_3$) When x = 0.54 and y = 0.04, a maximum value of d33 = 73 pC/N was finally reached. [101]

Finally, in order to improve the reaction kinetic of the KNN formation and further reduce the synthesise time, the hydrothermal approach can be combined with microwave heating. [102, 103] Temperature below 200°C and annealing time lower than 7 hours allow to obtain crystalline KNN systems and avoid secondary phases typically produced under prolonged dwell time and high processing temperatures (>600 °).

The piezoelectric properties and the parameters related with synthesis of KNN by wet-chemistry are summarized in Table 3.

3. Conclusions and Future Perspectives.

The technological opportunities connected with the utilization of lead-free KNN piezoceramics in advanced area of ultrasonic transducers for biomedical devices, is a primary source of interest, and the opportunity to replace conventional PZT with KNN-based materials in these instruments, is attracting the attention of an increasing number of scientists.

More generally, since its discovering in the late 1954, the interest in the investigation of KNN-based materials has considerably increased. In particular, the number of publications concerning this subject have seen an exponential growth from about 3 in 2000 to 250 in 2016, which can be clearly appreciated by the bar plots reported in Figure 12.

This fervent interest is also corroborated by the high percentage (50%) of manuscripts regarding alkali niobates with respect to the study devoted to lead-free systems in the last 10 years. Initially, the studies were most focused on the pure $K_xNa_xNbO_3$ system, whereas today the number of papers concerning KNN-doped materials is significantly greater. The explanation for this trend can be found in the impellent necessity to obtain lead-free systems with piezo properties comparable with the classical PZT. In fact, as emerged by the literature reviewed in this work, a strong difference of d_{33} is shown between an un-doped (110 pC/N) and doped (490 pC/N) KNN systems, both prepared by conventional route. [44, 63] In this direction, for better analyzing the data reported in Table 1, the piezoelectric activity, reported as d_{33} constant, versus the electromechanic coupling coefficient, which represents the piezoelectric efficiency, is plotted for different KNN-doped materials in Figure 13.

Depending on the dopant that it contains, the KNN system shows different properties. The additives based on metal oxides (green panel, Figure 13), extensively studied during the last 20 years, present feeble improvement if compared with the un-doped sample. An important enhancement is produced when composites are used (blue and orange panels). In particular, systems doped with different percentage of Sb_xO_3-0.04$BaZrO_3$ (orange panel), show a very high piezoelectric constant similar to soft PZT (~500 pC/N). It is believed that one of the principal effect of these dopants is to shift the polymorphic phase boundary (T_{O-T}) to room temperature, then improving the piezoelectric properties. This has the cost of the thermal in-stability of the properties and opens a, yet unexplored, research path for stability enhancement of the materials.

The most promising systems reported in Figure 14, have been tested as active material in ultrasonic transducer prototypes. Together with the piezoelectric activity, the sensitivity and the frequency at which the transducers operate, play a crucial role in the transducer performance. The properties of the materials,

reported in Table 2, seems to match some of the market targets (see Figure 14), although further improvements are still required. In this context, several studies, mostly exploring new synthetic routes have been gradually combined with the investigations of the structure-property relationships of the KNN-based systems. Among the numerous synthetic strategies used for KNN fabrication, the solid state and the crystal growth routes represents the most exploited for ultrasonic purpose. However, in the last 5 years, the KNN systems prepared by wet-chemical approaches increased significantly. The temperatures involved (see table 3) are in fact lower with respect to the conventional routes, guarantying a good control of the stoichiometric and, in most of the case, pure phases. Not less important, wet-chemistry routes allow to prepare KNN based materials in different shape and size, ranging from thin films, suitable for miniaturized devices, to several grams of powders scalable to industrial purpose. For these reasons, it is expected a significant impact of this technique also for ultrasonic transducers in a near future. The need to tune the physical and chemical properties in connection with the microscopic structure of KNN systems is perceived, in fact, as a central challenge for improving the properties of these materials. Furthermore, controlled porosity can be induced in the KNN system using soft-chemistry approach. This could result very useful for creating piezo transducer for ultrasound application by coupling dense (active layer) and interconnected porous ceramics (matching layer), as summarized in Figure 15. This strategy has been successfully exploited in the PZT systems, with a sensible improvement of the acoustic properties of the ceramics. However, apart few studies on macroporous KNN systems, no data are available for highly-ordered and disordered mesoporous KNN materials. These systems should be characterized by an elevated surface area and the nanosized pores would further decrease the acoustic impedance of the ceramic materials. Based on these considerations, more efforts have to be addressed not only on the studies of new synthesis of mesoporous KNN, but also on a detailed characterization of their acoustic properties undervalued in the current studies.

Consequent to the large number of experimental variables, such as solvents, reagents, temperatures, pH, stabilizers, etc., further investigations are necessary to find appropriate conditions for the fabrication of optimized KNN ceramics used in ultrasonic transducer. One of the most crucial point regards the choice

of the reagents and corresponding solvents. As emerged in Table 3, different families of metallic precursors have been tested: nitrate, carbonate, oxide, hydroxide and acetate based metals (K, Na and Nb) are probably the most explored. Regarding the solvents, the principal issue to be overcome corresponds to the solubility differences among the three metal-based reagents present in the initial solution. The poor solubility of one reagent respect to the others can lead to side reactions with secondary phases and undesired stoichiometry of the final systems. Another problem is the reagents precipitation during the sol-gel synthesis. To avoid that, chelating agents, such as acetic acid, 2-methoxyethanol, and acetylacetone, are introduced to stabilize the metal ions in the solutions. This strategy is typically used in the presence of potassium and sodium acetates and carbonates. However, although the promising results achieved, in the last years the use of hydroxides as starting reagents has gained increasing attentions. This because, water can be used as solvent avoiding more toxic and expensive solvents. For a rapid penetration into the global market, it is in fact very important that these new synthetic approaches will assure enhanced properties of the final materials prepared by cheaper and "greener" raw materials. Finally, in a medium-term perspective, along with the improved control of the experimental conditions for the synthesis of highly functional KNN materials, important progresses have been surely made on the manufacture of the transducers. In particular, the coupling of the active and matching layers, the definite choice of the working electrodes and the backing substrate material, represent important aspects for developing innovative ultrasonic transducers.

Acknowledgment: This work has been funded by the H2020-MSCA-IF-2015 grant number #707954. All the Authors contributed equally to this work. Dr. Sebastiano Garroni, Nina Senes, Antonio Iacomini realized the structure design of the manuscript together with Prof. Lorena Pardo and Santiago Cuesta-Lopez. Prof. Stefano Enzo and Prof. Gabriele Mulas contributed to the writing and revision of the review.

References:

[1]. J. Holterman, P. Groen, *an introduction to Piezoelectric Materials and Applications*, first ed., Stichting Applied Piezo, Apeldoorn, **2013.**

[2]. Market Report, Global Piezoelectric Device Market, January, 2017, Publisher: Acmite Market Intelligence, Language: English, Pages: 543.

[3]. Q. Zhou, K. H. Lam, H. Zheng, W. Qiu, K. K. Shung, Prog. *Mater. Sci*. **2014,** 66, 87.

[4]. H. Chabok, C. Zhou, Y. Chen, A. Eskandarinazhad, Q. Zhou and K. Shung, Ultrasound Transducer Array Fabrication Based on Additive Manufacturing of Piezocomposites, Proceedings of the ASME 2012 International Symposium on Flexible Automation ISFA2012, ISFA2012-7119, 433-444.

[5]. E. Mercadelli, A. Sanson, C. Galassi., Book chapter: Porous Piezoelectric Ceramics, Piezoelectric Ceramics, Ernesto Suaste-Gomez (ed.), InTech 2010, 111-128.

[6]. K. Boumchedda, M. Hamadi, G. Fantozzi, *J. Eur.Ceram.Soc*. **2007**, 27, 4169.

[7]. E. Taghaddos, M. H. Hejazi, A. Safari, *J. Adv. Dielect.* **2015**, 5, 1530002.

[8]. J.F. Li, K. Takagi, M. Ono, W. Pan, R. Watanabe, A. Almajid, M. Taya, *J. Am. Ceram. Soc*. **2003**, 86, 1094.

[9]. S. Geis, P. Löbmann, S. Seifert, J. Fricke, *Ferroelectrics*, **2000**, 241, 1719.

[10]. C.R Bowen, A. Perry, A.C.F. Lewis, H. Kara, *J. Eur. Ceram. Soc*. **2004,** 24, 541.

[11]. A. Yang, C.-A. Wang, R. Guo, Y. Huang, C.-W. Nan, *J. Am. Ceram. Soc*. **2010,** 93, 1427.

[12]. R.A. White, J.N. Weber, E.W. White, *Science*. **1972**, 176, 922.

[13]. A.R. Studart, U.T. Gonzenbach, E. Tervoort, L.J. Gauckler, *J. Am. Ceram. Soc*. **2006**, 89, 1771.

[14]. F. Lionetto, A. Licciulli, F. Montagna, A. Maffezzoli, *C e Ca*. **2004**, 34, 107.

[15]. Y. Saito, H. Takao, Toshihiko Tani, T. Nonoyama, K. Takatori, T. Homma, T. Nagaya, M. Nakamura, *Nature*. **2004**, 432, 84.

[16]. C.-H. Hong, H.-P. Kim, B.-Y. Choi, H.-S. Han, J. S. Son, C. W. Ahn, W. Jo, *J. Materiomics*. **2016**, 2, 1.

[17]. M. E. Villafuerte-Castrejón, E. Morán, A. Reyes-Montero, R. Vivar-Ocampo, J.-A. Peña-Jiménez, S.-O. Rea-López, L. Pardo, *Materials*. **2016**, 9(21), 1.

[18]. EU-Directive 2002/95/EC: Restriction of the use of certain hazardous substances in electrical and electronic equipment (RoHS), Offic. *J. Europ. Union.* **46** L37 (2003), 19-23.

[19]. J. Rodel, W. Jo, K. T. P. Seifert, E.-M. Anton, T. Granzow, D. Damjanovic, *J. Am. Ceram. Soc.* **2009,** 92**,** 1153.

[20]. X. Cheng, J. Wu, X. Wang, B. Zhang, J. Zhu, D. Xiao, X. Wang, X. Lou, *Appl. Phys. Lett*. **2013**, 103, 052906.

[21]. H. Yamada, T. Matsuoka, H. Kozuka, M. Yamazaky, K. Ohbayashi, T. Ida, *J. Appl. Phys*. **2015**, 117, 214102.

[22]. X. Cheng, Q. Gou, J. Wu, X. Wang, B. Zhang, D. Xiao, J. Zhu, X. Wang, X. Lou, *Ceram. Int*. **2014**, 40, 5771.

[23]. N. Yin, A. Jalalian, L. Zhao, Z. Gai, Z. Cheng, X. Wang, *J. Alloy. Compd*. **2015**, 652, 341.

[24]. J. Rödel, K. G. Webber, R. Dittmer, W. Jo, M. Kimura, D. Damjanovic, *J. Eur. Ceram. Soc*. **2015**, 35, 1659.

[25]. A. Safari, E.K. Akdogan, *Piezoelectric and Acoustic Materials for Transducer Applications*, Springer Science&Business Media, Academic, New York, **2008**.

[26]. K. Momma, F. Izumi, *J. Appl. Crystallogr.* **2011**, 44**,** 1272.

[27]. P. Dubernet, J. Ravez, *Ferroelectrics*. **1998**, 211(1), 51.

[28]. J. Wu, D. Xiao, *Appl. Phys. Lett*. **2007**, 91(25), 252907.

[29]. L. Egerton, D. M. Dillon, *J. Am. Ceram. Soc*. **1959**, 42(9), 438.

[30]. B. Jaffe, W. Cook, H. Jaffe, *Piezoelectric Ceramics*, Academic Press, London and New York, **1971**.

[31]. B. Malič, J. Koruza, J. Hreščak, J. Bernard, K. Wang, J. G. Fisher, A. Benčan, *Materials*. **2015**, 8(12), 8117.

[32]. M. Kosec, D. Kolar, *Mater. Res. Bull*. **1975**, 10(5), 335.

[33]. M. Matsubara, T. Yamaguchi, K. Kikuta and S. Hirano, *JPN J. Appl. Phys.* **2005**, 44(1A), 258.

[34]. R. Zuo, J. Rödel, R. Chen, L. Li, *J. Am. Ceram. Soc*. **2006**, 89(6), 2010.

[35]. M. Ahtee, A. M. Glazer, *Acta Crystallogr. A: Foundations of Crystallography*. **1976**, 32, 434.

[36]. M. Ahtee and A. W. Hewat, *Acta Crystallogr. A: Foundations of Crystallography*. **1978**, 34, 309.

[37]. Y. L. Qin, J. L. Zhang, W. Z. Yao, C. J. Lu, S. J. Zhang, *ACS Appl. Mater. Interfaces*. **2016**, 8, 7257.

[38]. F. R. Marcos, R. López-Juárez, R. E. Rojas-Hernandez, A. del Campo, N. Razo-Pérez, J. F. Fernandez, *ACS Appl. Mater. Interfaces*. **2015**, 7, 23080.

[39]. X. Wang, J. Wu, D. Xiao, J. Zhu, X. Cheng, T. Zheng, B. Zhang, X. Lou, X. Wang, *J. Am. Chem. Soc*. **2014**, 136(7), 2905.

[40]. X. Cheng, J. Wu, X. Wang, B. Zhang, X. Lou, X. Wang, D. Xiao, J. Zhu, *ACS Appl. Mater. Interfaces*. **2013**, 5(21), 10409.

[41]. R. Zuo, J. Fu, *J. Am. Ceram. Soc*. **2011**, 94(5), 1467.

[42]. Y. Guo, K. Kakimoto, H. Ohsato, *Mater. Lett*. **2005**, 59(2-3), 241.

[43]. S. Priya, S. Nahm, *Lead-free piezoelectrics*, Springer, **2013**.

[44]. J. Wu, D. Xiao, J. Zhu, *Chem. Rev*. **2015**, 115(7), 2559.

[45]. H. Birol, D. Damjanovic, N. Setter, *J. Eur. Ceram. Soc*. **2006**, 26, 861.

[46]. R. Zuo, M. Wang, B. Ma, J. Fu, T. Li, *J. Phys. Chem. Solids*. **2009**, 70(3–4), 750.

[47]. R. Zuo, J. Rödel, R. Chen, L. Li, *J. Am. Ceram. Soc*. **2006**, 89(6), 2010.

[48]. M.R. Yang, C.-C. Tsai, C.-S. Hong, S.-Y. Chu, S.-L. Yang, *J. Appl. Phys*. **2010**, 108(9), 94103.

[49]. S. Su, R. Zuo, X. Wang, L. Li, *Mater Res. Bull*. **2010**, 45(2), 124.

[50]. D. Lin, M. S. Guo, K. H. Lam, K. W. Kwok, H. L. W. Chan, *Smart Mater. Struct.* **2008**, 17(3), 35002.

[51]. B. C. Park, I. K. Hong, H. D. Jang, V. D. N. Tran, W. P. Tai, J.-S. Lee, *Mater. Lett*. **2010**, 64(14), 1577.

[52]. J. Bernard, A. Benčan, T. Rojac, J. Holc, B. Malič, *J. Am. Ceram. Soc*. **2008**, 91, 2409.

[53]. H.-C. Song, K.-H. Cho, H.-Y. Park, C.-W. Ahn, S. Nahm,, K. Uchino, S.-H. Park, H.-G- Lee, H, *J. Am. Ceram. Soc*. **2007**, 90, 1812.

[54]. K. Wang, J. F. Li, N. Liu, *Appl. Phys. Lett*. **2008**, 93(9), 3.

[55]. H. Du, W. Zhou, F. Luo, D. Zhu, S. Qu, Y. Li, Z. Pei, *J. Phys. D Appl. Phys*. **2008**, 41(8), 85416.

[56]. D. Lin, K. W. Kwok, H. W. L. Chan, *Appl. Phys. Lett*. **2007**, 91(14), 143513.

[57]. Z. Chen, X. He, Y. Yu, J. Hu, *Jpn. J. Appl. Phys*. **2009**, 48(3), 30204.

[58]. C. Zhang, Z. Chen, W. Ji, L. Wang, Y.B. Chen, S.-H. Yao, S.-T. Zhang, Y.-F. Chen, *J. Alloy. Compd*. **2011**, 509(5), 2425.

[59]. B. Zhang, J. Wu, X. Cheng, X. Wang, D. Xiao, J. Zhu, X. Wang, X. Lou, *ACS Appl. Mater. Interfaces*. **2013**, 5(16), 7718.

[60]. X. Cheng, J. Wu, X. Wang, B. Zhang, J. Zhu, D. Xiao, X. Wang, X. Lou, *Appl. Phys. Lett*. **2013**, 103(5), 052906.

[61]. M. Bah, F. Giovannelli, R. Retoux, J. Bustillo, E. Le Clezio, I. Monot-Laffez, *Cryst. Growth Des*. **2016**, 16(1), 315.

[62]. Y. Chen, W.B. Qiu, K.H. Lam, B.Q. Liu, X.P. Jiang, H.R. Zheng, H.S. Luo, H.L.W. Chan, J.Y. Dai, *Ultrasonics*. **2015**, 56, 227.

[63]. J. Ou-Yang, B. Zhu, Y. Zhang, S. Chen, X. Yang, W. Wei, *Appl. Phys A- Mater*. **2015**, 118(4), 1177.

[64]. N. M. Hagh, B. Jadidian, E. Ashbahian, A. Safari, *IEEE T. Ultrason. Ferr*. **2008**, 55(1), 214.

[65]. X. Huo, L. Zheng, R. Zhang, R. Wang, J. Wang, S. Sang, Y. Wang, B. Yanga, W. Cao, *Cryst. Eng. Comm*. **2014**, 16(42), 9828.

[66]. X. Huo, L. Zheng, S. Zhang, R. Zhang, G. Liu, R. Wang, B. Yang, W. Cao, T. R. Shrout, *Phys Status Solidi-RRL*, **2014**, 8(1), 86.

[67]. D.W. Wu, R.M. Chen, Q.F. Zhou, K.K. Shung, D.M. Lin, H.L.W. Chan, *Ultrasonics*. **2009**, 49(3), 395.

[68]. H. Tian, C. Hu, X. Meng, Z. Zhou, G. Shi, *J. Mater. Chem. C*. **2015**, 3(37), 9609.

[69]. F. Levassort, J. Gregoire, M. Lethiecq, K. Astafiev, L. Nielsen, R. Lou-Moeller, W. W. Wolny, *IEEE Inter. Ultra. Sym*. **2011**, 848.

[70]. Z. Shen, J.-F. Li, R. Chen, Q. Zhou, K.K. Shung, *J. Am. Ceram. Soc*. **2011**, 94(5), 1346.

[71]. R. López-Juárez, F. González-García, J. Zárate-Medinac, R. Escalona-González, S. Díaz de la Torre, M.-E. Villafuerte-Castrejóna, *J. Alloy. Compd*. **2011**, 509, 3837.

[72]. R. López, F. González, M.E. Villafuerte-Castrejón, *J. Eur. Ceram. Soc*, **2010**, 30, 1549.

[73]. M. Dolhen, A. Mahajan, R. Pinho, M. E. Costa, G. Trolliard, P. M. Vilarinho, *RSC Adv*. **2015**, 5(6), 4698.

[74]. K. H. Lam, H. F. Ji, F. Zheng, W. Ren, Q. Zhou, K. K. Shung, *Ultrasonics*. **2013**, 53(5), 1033.

[75]. R. Gao, X. Chu, Y. Huan, X. Wang, L. Li, *Phys. Status Solidi A*. **2014**, 211(10), 2378.

[76]. D. Zhang, F. Zheng, X. Yang, L. Feng, X. Huang, H. Liu, M. Cao, *Integr. Ferroelectr*. **2014**, 154(1), 97.

[77]. H. Brunckova, L. Medvecký, P. Hvizdoš, J. Ďurišin, *Surf. Interface Anal*. **2015**, 47(11), 1063.

[78]. K. I. Kakimoto, T. Imura, Y. Fukui, M. Kuno, K. Yamagiwa, T. Mitsuoka, K. Ohbayashi, *Jpn. J. Appl. Phys*. **2007**, 46(10B), 7089.

[79]. Y. Xu, D. Liu, F. Lai, Y. Zhen, J.-F. Li, *J. Am. Ceram. Soc*. **2008**, 91(9), 2844.

[80]. F. Söderlind, P.-O. Käll, U. Helmersson, *J. Cryst. Growth*. **2005**, 281(2–4), 468.

[81]. A. Chowdhury, S. O'Callaghan, T. A. Skidmore, C. James, S. J. Milne, *J. Am. Ceram Soc*. **2009**, 92(3), 758.

[82]. Y. Cao, K. Zhu, H. Zheng, J. Qiu, H. Gu, *Particuology*. **2012**, 10(6), 777.

[83]. Gh.H. Khorrami, A. Kompany, A. Khorsand Zak, *Mater. Lett*. **2013**, 110, 172.

[84]. Gh. H. Khorrami, A. Kompany, A. Khorsand Zak, *Adv. Powder Technol*. **2015**, 26(1), 113.

[85]. D.-Q. Zhang, Z.-C. Qin, X.-Y. Yang, H.-B- Zhu, M.-S. Cao, *J. Sol-Gel Sci. Techn*. **2011**, 57(1), 31.

[86]. C. Wang,Y.-D. Hou, H.-Y. Ge, M.-K. Zhu, H. Yan, *J. Eur. Ceram. Soc*. **2010**, 30(7), 1725.

[87]. A. Jalalian, A. M. Grishin, *Appl. Phys. Lett*. **2012**, 100(1), 12904.

[88]. A. Jalalian, A. M. Grishin, *Appl. Phys. Lett.* **2014**, 104(24), 243701.

[89]. H. B. Kang, J. Chang, K. Koh, L. Lin, Y. S. Cho, *ACS Appl. Mater. Interfaces*. **2014**, 6(13), 10576.

[90]. J. Fang, X. Wang, L. Li, *Phys. Status Solidi-R*. **2012**, 6(3), 132.

[91]. Q. Yu, Jing-Feng Li, W. Sun, Z. Zhou, Y. Xu, Z.-K. Xie, F.-P. Lai1, Q.-M. Wang, *J. Appl. Phys*. **2013**, 113(2), 24101.

[92]. Q. Yu, J.-F. Li, Y. Chen, L.-Q. Cheng, W. Sun, Z. Zhou, Z. Wang, *J. Am. Ceram. Soc*. **2014,** 97(1), 107.

[93]. A. F. Solarte, N. Pellegri, O. de Sanctis, M. G. Stachiotti, *J. Sol-Gel Sci. Techn*. **2013**, 66(3), 488.

[94]. S. Wiegand, S. Flege, O. Baake, W. Ensinger, *J. Mater. Sci. Technol*. **2013**, 29(2), 142.

[95]. L.-L. Yao, L.-X. Ji, K.-J. Zhu, J. Wang, J.-S. Liu, J.-H. Qiu, *Energy Harvesting and Systems*. **2015**, 2, 149.

[96]. L.-L. Yao, K. Zhu, *Mod. Phys. Lett. B*. **2016**, 30(13), 2.

[97]. M.H. Maziati Akmal, A.R.M. Warikh, U.A.A. Azlan, M.A. Azam, S. Ismail, *Mater. Lett*. **2016**, 170, 10.

[98]. M. Zheng, Y. Hou, L. Zhang, M. Zhu, *Eur. J. Inorg. Chem*. **2016**, 19, 3072.

[99]. L. A. Ramajo, F. Rubio-Marcos, A. Del Campo, J. F. Fernández, M. S. Castro, R. Parra, *Ceram. Int*. **2014,** 40, 14701.

[100]. L. Ramajo, F. Rubio-Marcos, A. Del Campo, J. F. Fernández, M. S. Castro, R. Parra, *J. Mater. Sci-Mater. El*. **2015**, 26(12), 9402.

[101]. W. X. Ma, X. H. Fu, W. H. Tao, L. Yang, G. Y. Cheng, L. P. Zhao, *Mater. Sci. Forum*. **2016**, 859 3.

[102]. R. López-Juáreza, R. Castañeda-Guzmánb, M.E. Villafuerte-Castrejón, *Ceram. Int*. **2014**, 40, 14757.

[103]. M. Zhang, M. Guo, Y. Zhou, *Int. J Appl. Ceram. Tec*. **2011**, 8, 591.

Figure captions

Figure 1. Different sequence modes used in medical ultrasound transducers a) Single Element. b) Linear Array c) Phased Array and d) Matrix array.

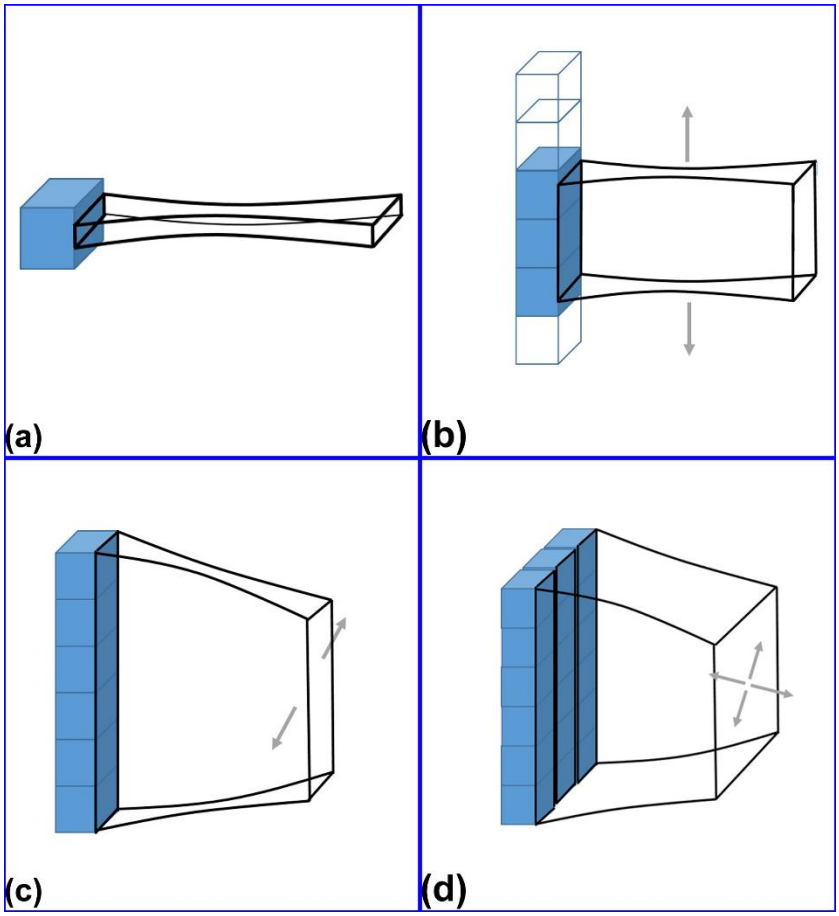

Figure 2. a) A new generation 4D probe for ultrasonic scanner. b) Schematic representation of a classical ultrasonic transducer.

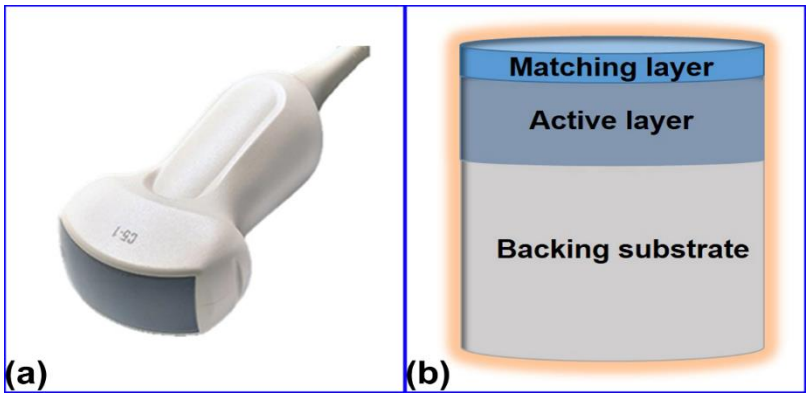

Figure 3. Orthorhombic perovskite structure on the $K_{0.5}Na_{0.5}NbO_3$ phase. K = purple; Na = yellow; Nb = green; O = red. [26]

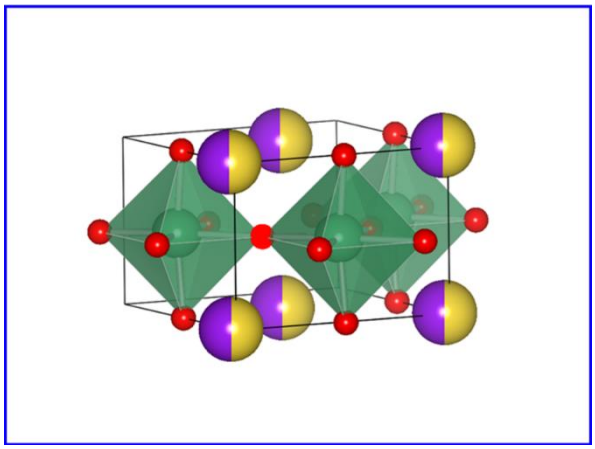

Figure 4. Schematic presentation of the mainly steps used in the production of KNN pellet by solid-state route. [1]

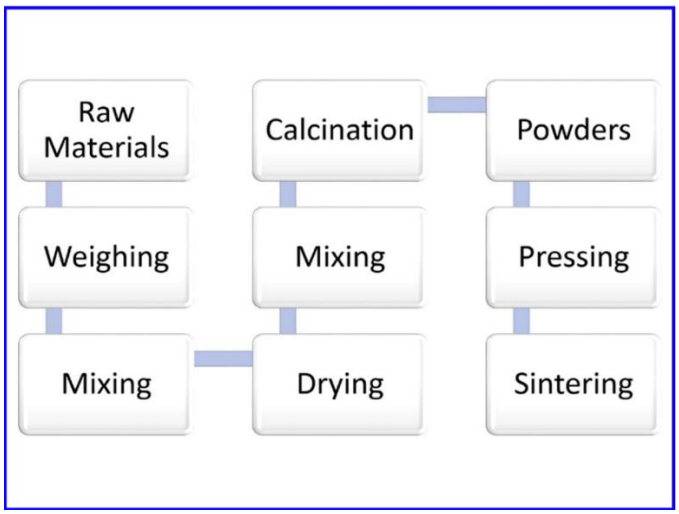

Figure 5. Configuration of the "top-seeded solution growth, TSSG" (a) and the "floating zone, FZM" (b) methods both used for producing large crystals.

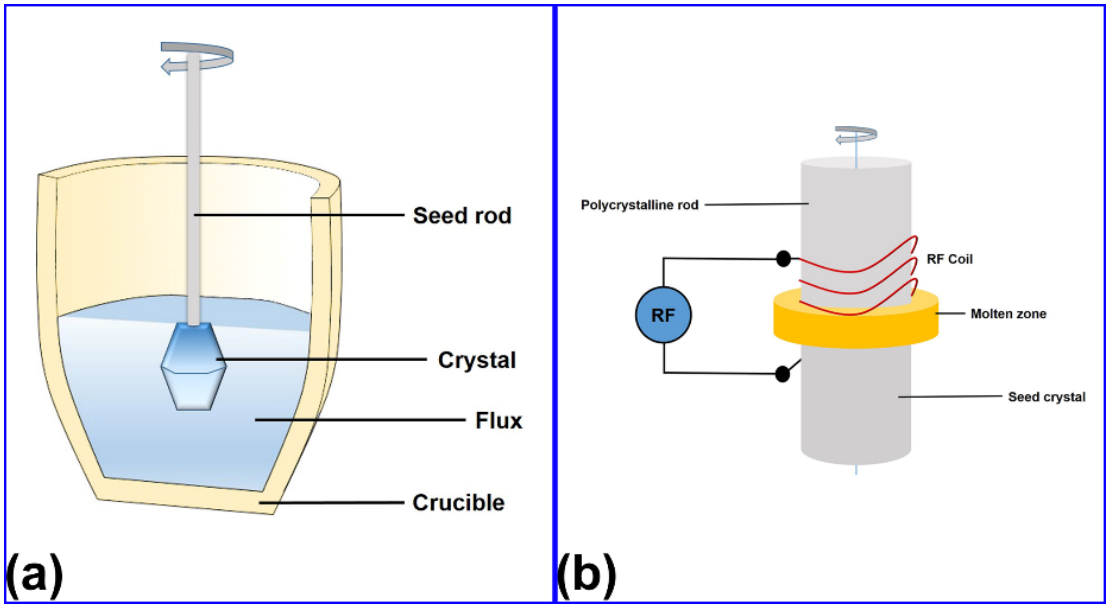

Figure 6. (a) Large crystal of KNN-Ta grown by FZM. [61] (b) KNN-TL single crystal grown by TSSG method. [65]

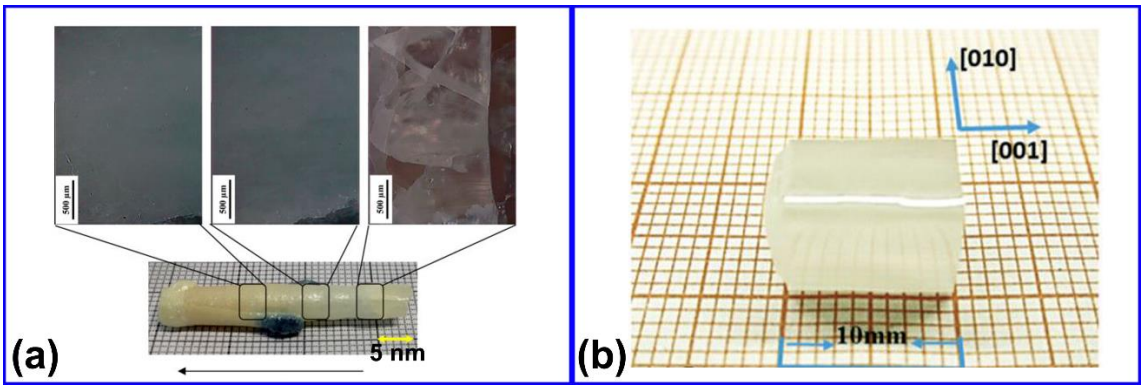

Figure 7. (a) Photograph of Li-, La-doped KNN transducer. [69] (b). Photograph of 1-3-type (NKLNT)/epoxy composite transducer. [70]

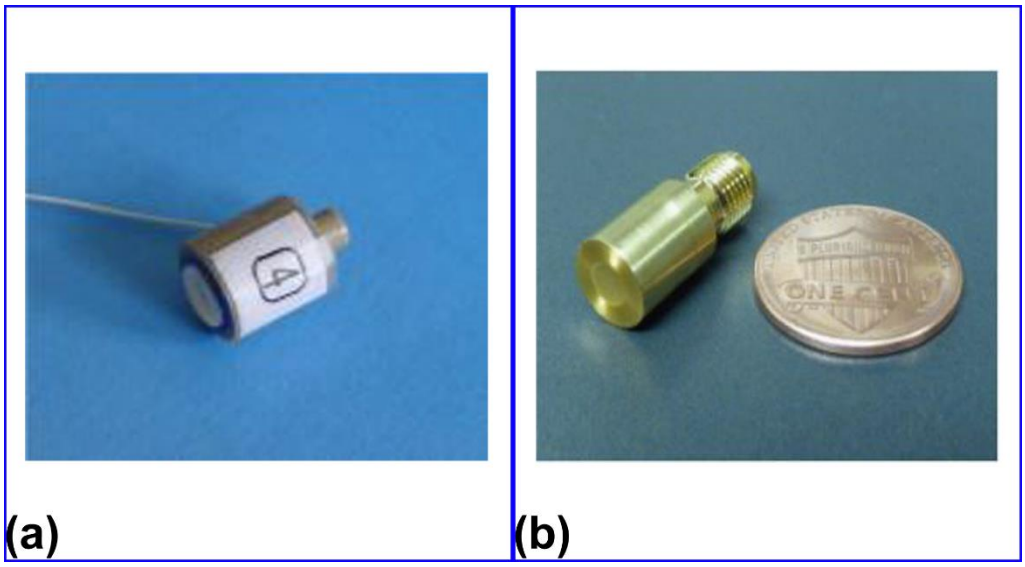

Figure 8. Schematization of the "spark plasma sintered, SPS" apparatus (a) and the "electrophoretic deposition, EDP" (b) method for preparing KNN thick films.

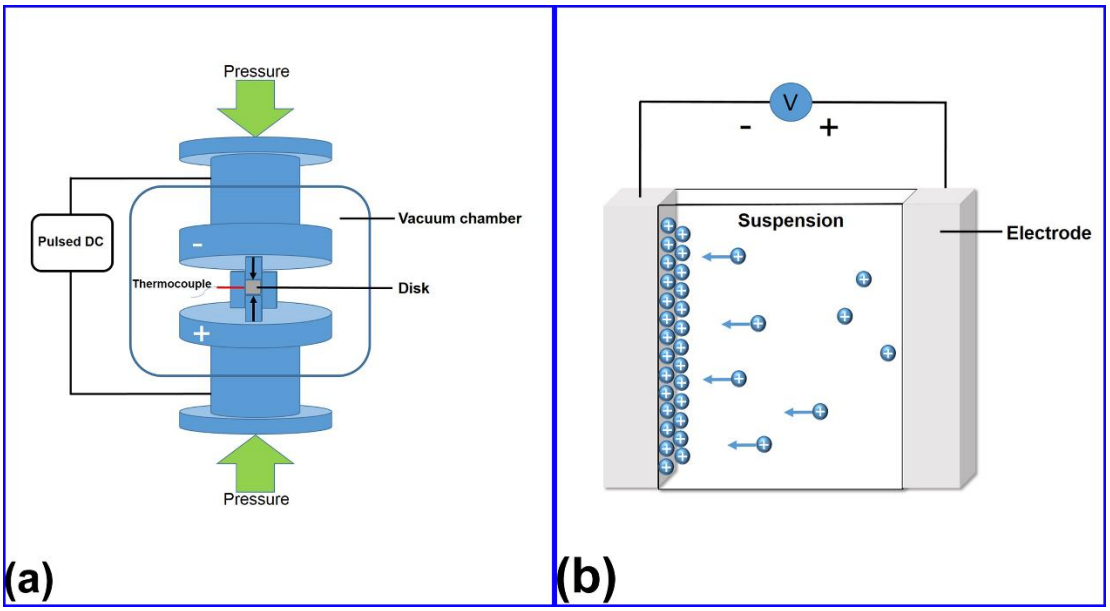

Figure 9. Sol gel synthesis routes scheme.

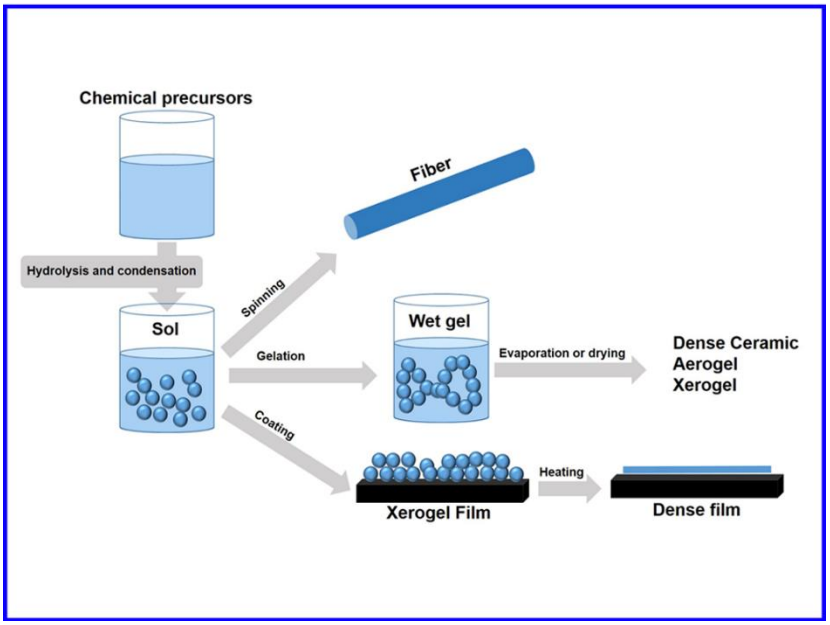

Figure 10. X-ray patterns of the KNN thin films prepared by method (a) I (600–900 °C), (b) II (700-900 °C) and (c) III (700-800°C). [80]

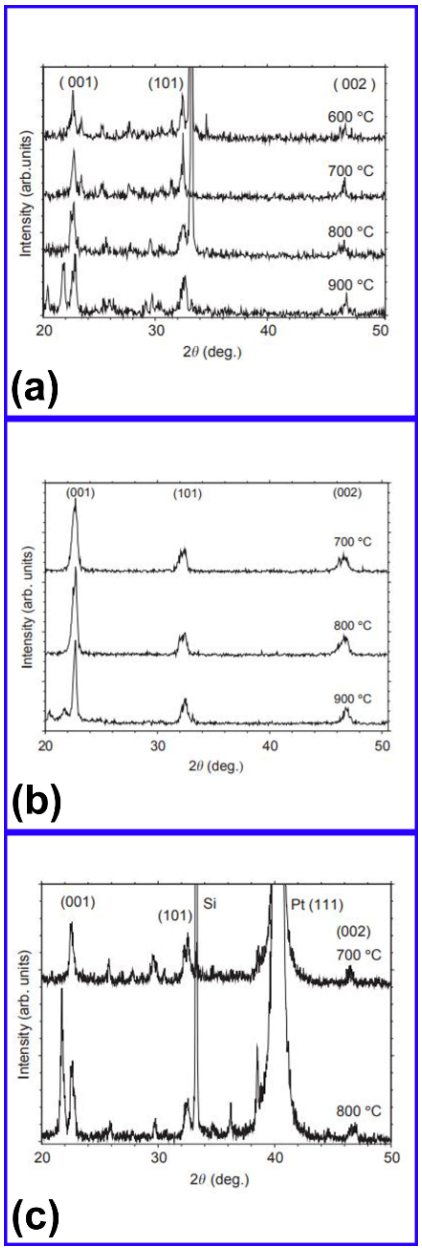

Figure 11. HR-TEM images of (a) un-doped and (b) Mn-doped (3.0%) KNN nanofibers. The corresponding SAED patterns and the piezoresponse amplitude of each fiber are displayed as inset. [89]

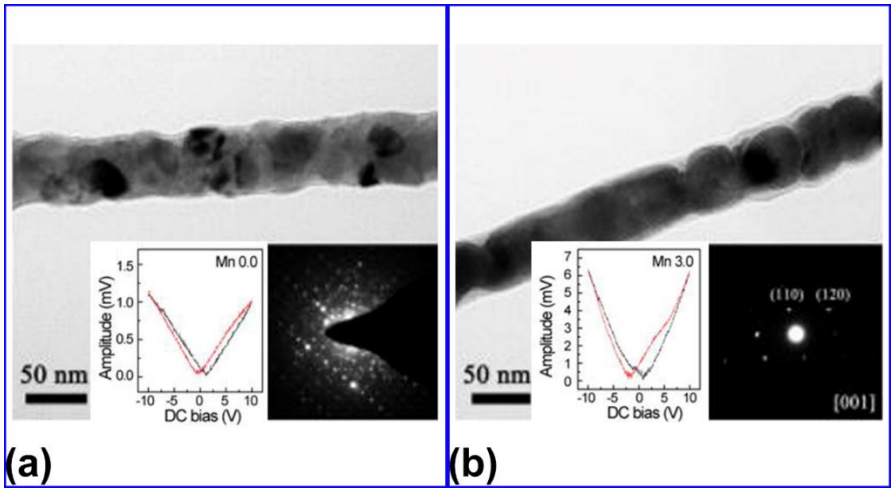

Figure 12. Number of publications (1950-2016) on potassium sodium niobate piezoceramics.

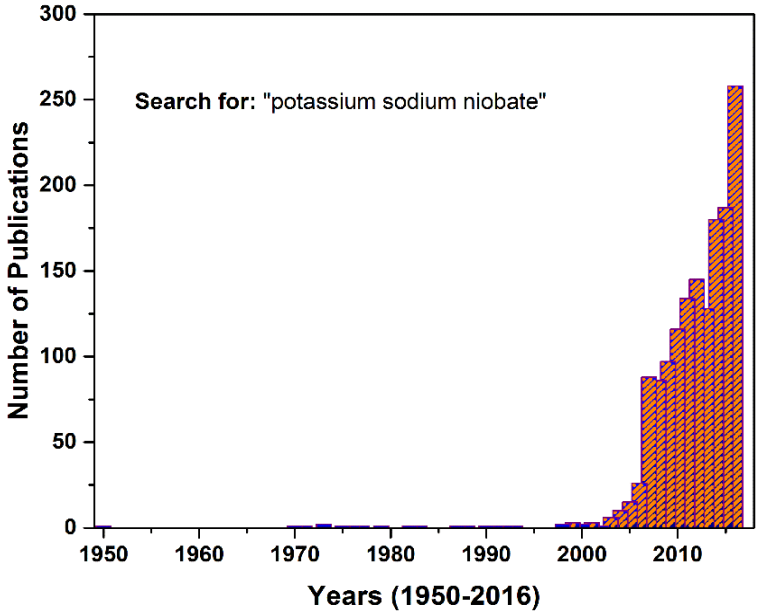

Figure 13. Figure 13. Piezoelectric activity, as evaluated by the value of the d_{33} piezoelectric coefficient, versus the planar electromechanic coupling coefficient (k) of thin disks for different KNN-based dense ceramics, extracted from references in Table 1.

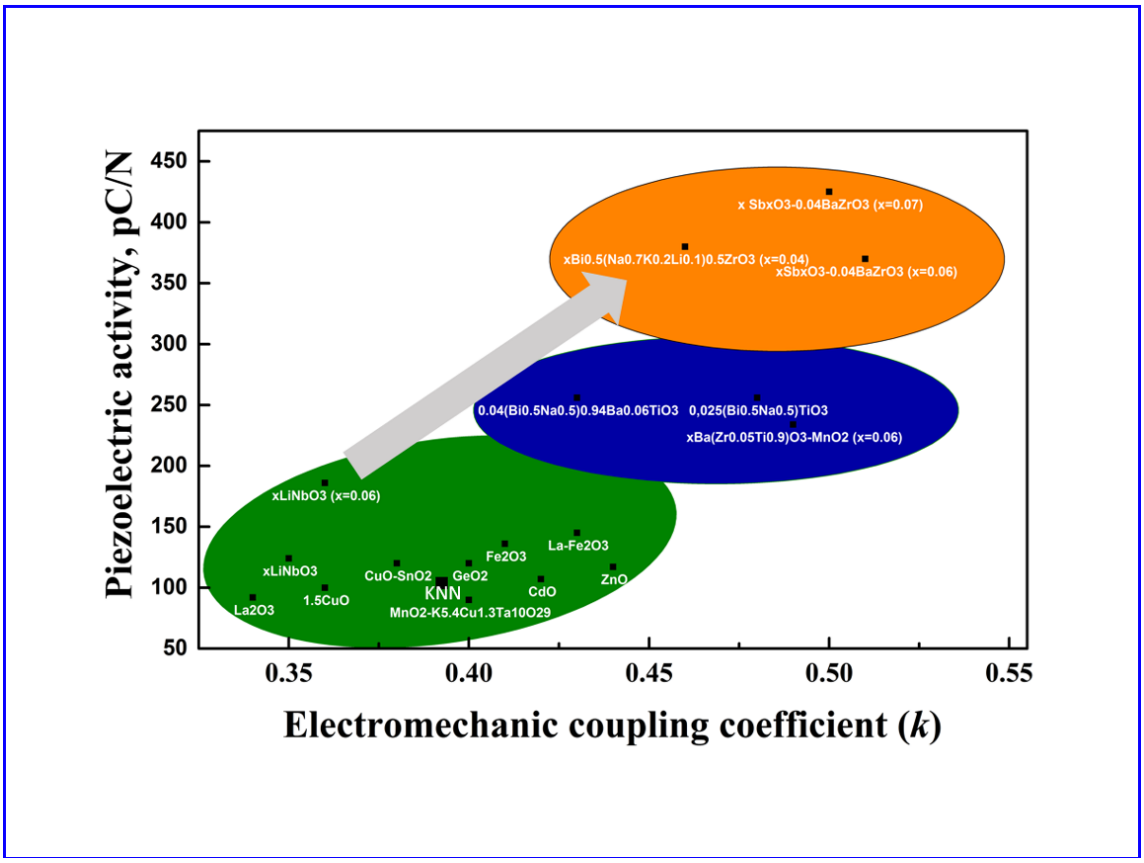

Figure 14. Piezoelectric activity, d_{33}, versus Frequency for different KNN-based ceramics prepared by different methods and tested in ultrasonic transducers. The values have been extracted from references in Table 2.

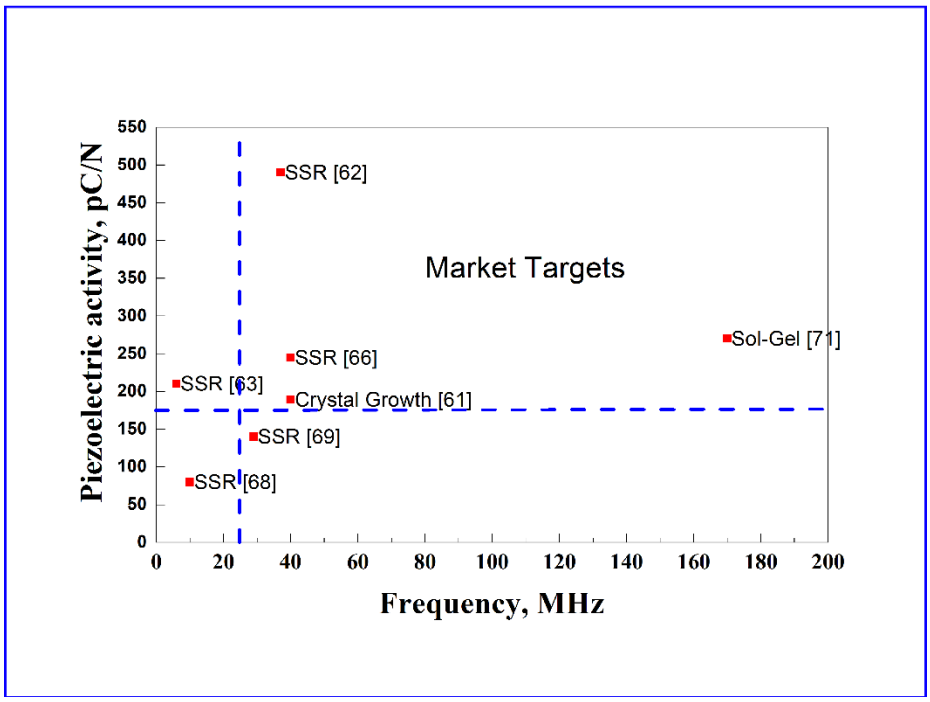

Figure 15. Scheme of the two preparation methods used to synthesize the active and matching layers in the new generation sensors.

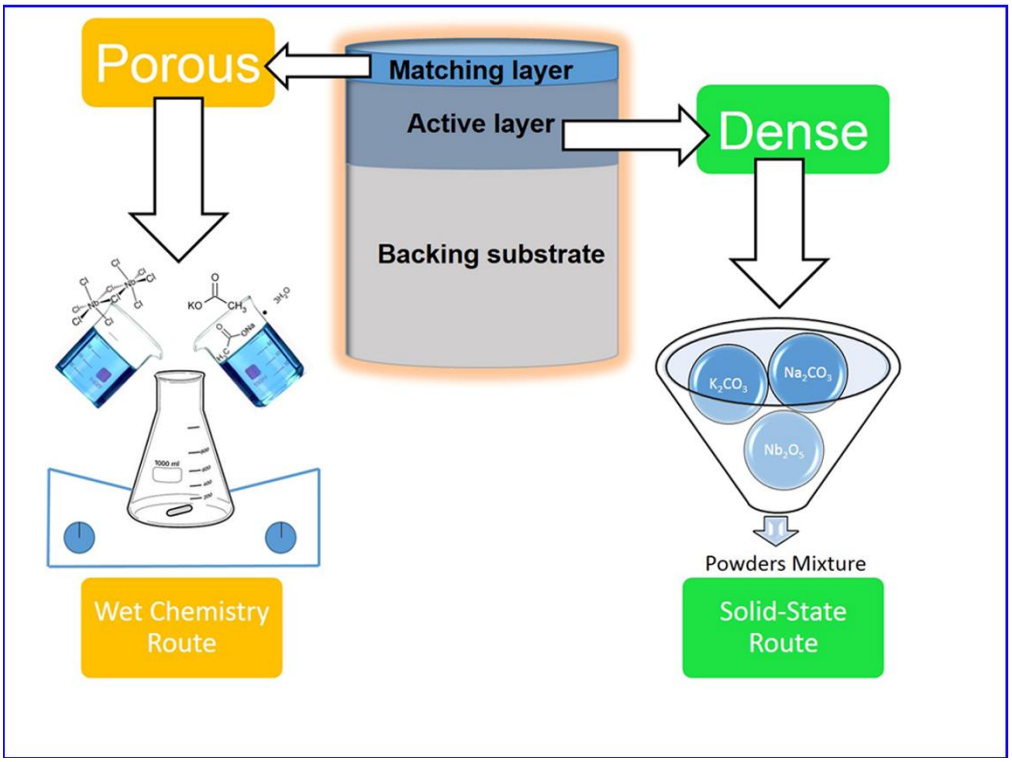

Table s

Table 1. Piezoelectric properties of the KNN dense systems and related compositions prepared conventional methods SSR.

Systems	Density (g/cm^3) or relative density	ε/ ε$_0$	d$_{33}$ (pC/N)	k$_p$	tan δ	Q$_m$	ref
KNLN-CuO	4.33	1287	109	0.36		1023	[43]
KNN-CuO	98.9%	237	96	0.39	0.0050	415	[44]
KNN	4.30	472	110	0.39	-	-	[45]
KNN-Fe_2O_3	97.5%	593	136	0.41	0.0420	412	[46]
KNN-La_2O_3	93.3	815	92	0.34	0.1790	396	[46]
KNN-(La-Fe_2O_3)	96.7%	723	145	0.43	0.0390	392	[46]
KNN-ZnO	97%	652	117	0.44	0.0333	-	[47]
KNN-SnO_2	98%	627	108	0.39	0.0456	-	[47]
KNN-CdO	95,3%	493	107	0.42	0.0404	-	[47]
KNN-$CuNb_2O_6$	4.47	-	92.5	0.40	-	1933	[48]
KNN-CuO-SnO_2	97.8%	710	120	0.38	0.0130	1040	[49]
KNN-MnO_2-$K_{5.4}Cu_{1.3}Ta_{10}O_{29}$	4.65	300	90	0.40	0.0030	1900	[50]
KNN-$K_{5.4}Cu_{1.3}Ta_{10}O_{29}$-CuO	97%	285	94	0.38	0.0018	3053	[51]
KNN+1.5CuO(mol%)	91%		100	0.36	-	1200	[51]
KNN-0.5GeO_2(mass %)	4.24	387	80	0.38	0.0400	59	[52]
KNN-1GeO_2(mass %)	4.31	397	120	0.40	0.0200	77	[52]
KNN-2GeO_2(mass%)	4.30	388	115	0.37	0.0200	76	[52]
(1-x)($Na_{0.535}K_{0.48}$)NbO_3 -x$LiNbO_3$ (x=0.08)	4.38		280	0.483	-	--	[53]
(1-x)KNN-x$LiNbO_3$ (x=0.05)	91.1%	518	124	0.347	-	-	[53]

(1-x)KNN-xLiNbO$_3$ (x=0.06)	90.6%	696	186	0.36	-	-	[54]
0,975($K_{0.5}Na_{0.5}$)NbO$_3$-0,025($Bi_{0.5}Na_{0.5}$)TiO$_3$	-	-	256	0.48	-	-	[55]
(1-x)($K_{0.5}Na_{0.5}$)NbO$_3$−xBa($Zr_{0.05}Ti_{0.9}$)O$_3$−MnO$_2$ (x=0.06)	-	1191	234	0.49	0.0120	-	[56]
0.96($Na_{0.5}K_{0.5}$)NbO$_3$−0.04($Bi_{0.5}Na_{0.5}$)$_{0.94}$Ba$_{0.06}$TiO$_3$	-	875	256	0.43	0.0260	-	[57]
0.99$K_{0.5}Na_{0.5}$NbO$_3$−0.01$Bi_{0.8}La_{0.2}$FeO$_3$	-	-	144	0.34	-	-	[58]
0.96($K_{0.5}Na_{0.5}$)$_{0.95}$Li$_{0.05}$Nb$_{1-x}$Sb$_x$O$_3$-0.04BaZrO$_3$ (x=0.06)	-	2376	370	0.51	0.0330	47	[59]
0.96($K_{0.5}Na_{0.5}$)$_{0.95}$Li$_{0.05}$Nb$_{1-x}$Sb$_x$O$_3$-0.04BaZrO$_3$ (x=0.07)	-	3157	425	0.50	0.0320	42	[59]
0.96($K_{0.5}Na_{0.5}$)$_{0.95}$Li$_{0.05}$Nb$_{1-x}$Sb$_x$O$_3$-0.04BaZrO$_3$ (x=0.08)	-	3212	320	0.37	0.0380	55	[59]
(1-x)($K_{0.48}Na_{0.52}$)($Nb_{0.95}Sb_{0.05}$)O$_3$-xBi$_{0.5}$($Na_{0.7}K_{0.2}Li_{0.1}$)$_{0.5}$ZrO$_3$ (x=0.04)	-	2180	380	0.46	0.0350	-	[60]

Table 2. KNN based materials in ultrasonic transducers: properties and synthesis routes.

Systems	Frequency (MHz)	Sensitivity (dB)	d_{33} (pC/N)	Preparation Method	ref
KNN-Mn / KNN-Ta	-	-	65-70	Floating Zone Method	[61]
$0.97K_{0.5}Na_{0.5}NbO_3$–$0.03(Bi_{0.5}K_{0.5})TiO_3$-xMnO (x=0.4%)	40	-6	189	Crystal Growth-Bridgman technique	[62]
$0.96(K_{0.48}Na_{0.52})(Nb_{0.95}Sb_{0.05})O_3$–$0.04Bi_{0.5}(Na_{0.82}K_{0.18})_{0.5}ZrO_3$	37	-16	490	Solid-state reaction	[63]
$K_{0.5}Na_{0.5}NbO_3$-$LiTaO_3$-$LiSbO_3$-1%mol Ba^{2+}	6	-20	210	Solis state reaction-Wet ball milling	[64]
$[Li_x(K_{1-y}Na_y)_{1-x}](Nb_{1-z}Ta_z)O_3$, x=0.06; y=0.22; z=0.15	-	-	354	Top-seeded solution growth method	[65]
$Li_x(K_zNa_{1-z})_{1-x}Nb_{1-y}Ta_yO_3$, x = 0.03–0.09, y = 0.05–0.15, z = 0.7–0.9	-	-	255	Top-seeded solution growth method	[66]
$(K_{0.5}Na_{0.5})_{0.97}Li_{0.03}(Nb_{0.9}Ta_{0.1})O_3$	40	-18	245	Solid state reactio-Wet ball milling	[67]
$K_{0.8}Na_{0.2}NbO_3$	-	-	110	Top-seeded solution growth method	[68]
$K_{0.5}Na_{0.5}NbO_3$	10	-6	80	Solid-state reaction pad-printing technique	[69]
$(Na_{0.535}K_{0.485})_{0.95}Li_{0.05}(Nb_{0.8}Ta_{0.2}O_3$/epoxy composite	29	-6	140	Solid-State reaction -Spark plasma technique	[70]

$K_{0.5}Na_{0.5}NbO_3$	-	-	40	Solid state reaction electro-phoretic deposition	[73]
$K_{0.5}Na_{0.5}NbO_3$/ $Bi_{0.5}Na_{0.5}TiO_3$	170-320	-50, -60	270	Solid state reaction /Sol gel	[74]
$(Na_{0.52}K_{0.44}Li_{0.04})(Nb_{0.89}Sb_{0.05}Ta_{0.06})O_3$	-	-	309	Solid state reaction	[75]

Table 3. Piezoelectric activity and synthesis parameters of several KNN based systems prepared by wet-chemistry route. HAC=acetic acid; 2-MOE=2-methoxyethano; ACAC=acetylacetone

Systems	$T_{calcination}$ (°C)	ε/ $ε_0$	d_{33}(pC/N)	Reagents	Solvents	ref
$K_{0.5}Na_{0.5}NbO_3$	500, 550, 600	280	-	CH_3COOK, CH_3COONa, $Nb(OH)_5$, $C_6H_8O_7$, PVP	water	[76]
$K_{0.65}Na_{0.35}NbO_3$	400	-	-	K_2CO_3, Na_2CO_3, Nb-tartrate complex	HAC, EtOH, ethylene glycol, n-propanol, 1,2-propanediol	[77]
$Li_{0.06}(K0.5Na_{0.5})_{0.094}NbO_3/KNbO_3$	450	243	192	KOC_2H_5, $Nb(OC_2H_5)_5$	2-MOE,	[78]
$K_{0.5}Na_{0.5}NbO_3$	400	-	-	KOC_2H_5, $NaOC_2H_5$, $Nb(OC_2H_5)_5$, ACAC	2-MOE, HAC,	[79]
$K_{0.5}Na_{0.5}NbO_3$	400	-	-	K_2CO_3, Na_2CO_3, Nb-tartrate complex	HAC, ethylene glycol, 1-propanol, 1,2-propanediol	[80]
$K_{0.5}Na_{0.5}NbO_3$	700	-	-	KNO_3, $NaNbO_3$, ($C_4H_4NNbO_9$ xH_2O), $C_6H_8O_7$,	water, ethylene glycol, NH_4OH	[81]
$K_{0.5}Na_{0.5}NbO_3$	500-900	-	-	K_2CO_3, Na_2CO_3, Nb_2O_5, $C_6H_8O_7$, EDTA,	Water, EtOH, NH_4OH, HF	[82]

$K_{0.5}Na_{0.5}NbO_3$	500-900	-	-	KNO_3, $NaNbO_3$, ($C_4H_4NNbO_9$ xH_2O), Gelatin type b	water	[83]
$K_{0.5}Na_{0.5}NbO_3$	600	-	-	KNO_3, $NaNbO_3$, ($C_4H_4NNbO_9$ xH_2O), Starch	water	[84]
$K_{0.5}Na_{0.5}NbO_3$	500-800	-	-	K_2CO_3, Na_2CO_3, Nb_2O_5, $C_2H_8N_2O_4$, $C_2H_2O_4$	Water, NH_4OH, HF	[85]
$K_{0.5}Na_{0.5}NbO_3$	330-480	685	56 pm/V	CH_3COOK, CH_3COONa, $Nb(OC_2H_5)_5$, PVP	2-MOE,	[86]
$K_{0.65}Na_{0.35}NbO_3$	From 600 to 800		76 pm/V	KOC_2H_5, $NaOC_2H_5$, $Nb(OC_2H_5)_5$, PVP	2-MOE	[87], [88]
$K_{0.5}Na_{0.5}NbO_3$ – x Mn X= 0, 0.5, 1.0, 3.0 mol%	750	-	40 pm/V	CH_3COOK, CH_3COONa, $(CH_3COO)Mn_4(H_2O)$ $Nb(OC_2H_5)_5$, PVP	2-MOE, HAC	[89]
$(Li_{0.04}K0_{.44}Na_{0.52})(Nb_{0.86}Ta_{0.06}Sb_{0.08})O_3$	600	-	311	$Nb(OH)_5$, $Ta(OC_2H_5)_5$, Sb_2O_3, K_2CO_3, Na_2CO_3, Li_2CO_3, $C_6H_8O_7$, $C_2H_2O_4$	Water, NH_4OH	[90]
$K_{0.5}Na_{0.5}NbO_3$	From 350 to 550	-	51 pm/V	KOC_2H_5, $NaOC_2H_5$, $Nb(OC_2H_5)_5$,	2-MOE	[91], [92]
$K_{0.5}Na_{0.5}NbO_3$ doped with Li and Ta	600-700	-	-	KOC_2H_5, $NaOC_2H_5$, $Nb(OC_2H_5)_5$	EtOH, acetoin	[93]

$K_{0.5}Na_{0.5}NbO_3$	600-700	-	-	CH_3COOK, CH_3COONa, $Nb(OC_2H_5)_5$,	1,3-propanediol, ACAC	[94]
$K_{0.6}Na_{0.5}NbO_3$	500	250	-	K_2CO_3, Na_2CO_3, Nb_2O_5, $C_6H_8O_7$	Water, HF, ethylene glycol	[95]
$K_{0.5}Na_{0.5}NbO_3$	450-550	-	-	CH_3COOK, CH_3COONa, Nb_2O_5, $C_6H_8O_7$	Water, HF, NH_4OH, 2-MOE	[96]
$K_{0.5}Na_{0.5}NbO_3$ – x Y X= 0, 0.1, 0.3, 0.5, 0.7, 0.9 mol%	200	-	-	CH_3COOK, CH_3COONa, $Nb(OC_2H_5)_5$, $Y(NO_3)_3 6H_2O$	2-MOE, ACAC	[97]
$(K_{0.5}Na_{0.5})_{0.094}Li_{0.06}NbO_3$ – x Mn X= 0-4.0 mol%	500	212	-	K_2CO_3, Na_2CO_3, $(CH_3COO)_2Mn$, Li_2CO_3, $C_6H_8O_7$,	Water, HAC	[98]
$K_{0.1}Na_{0.9}NbO_3$	190	176	-	NaOH, KOH, Nb_2O_5	Water	[99]
$K_{0.1}Na_{0.9}NbO_3$, $K_{0.65}Na_{0.35}NbO_3$	200	-	45-61	NaOH, KOH, Nb_2O_5, CTAB, HMTA, Triton X-100	Water	[100]
$K_{0.46}Na_{0.54}Nb_{0.95}Sb_{0.05}O_3$	200	73	-	NaOH, KOH, Nb_2O_5, Sb_2O_5	Water	[101]